

# Small scale autonomous watercraft for aquatic mapping

Cite as: AIP Conference Proceedings **2233**, 020015 (2020); <https://doi.org/10.1063/5.0001371>  
Published Online: 05 May 2020

Kit Hong Lee, Swee King Phang, and Yen Myan Felicia Wong



View Online



Export Citation

Lock-in Amplifiers  
up to 600 MHz



# Small Scale Autonomous Watercraft for Aquatic Mapping

Kit Hong Lee<sup>1</sup>, Swee King Phang<sup>1,a)</sup>, Yen Myan Felicia Wong<sup>1</sup>

<sup>1</sup>*School of Engineering, Taylor's University, 1 Jalan Taylor's, 47500, Subang Jaya, Selangor, Malaysia.*

<sup>a)</sup> *Corresponding author: [sweeking.phang@taylors.edu.my](mailto:sweeking.phang@taylors.edu.my)*

**Abstract.** Aquatic mapping or bathymetric mapping in small and shallow waterbodies is a challenging task using conventional bathymetric surveying techniques. In this paper, a small scale multi-hulled watercraft equipped with navigational sensors is developed for autonomous in situ bathymetric data collection using a single beam echosounder (SBES) has been produced. This paper describes the methodology in the integration of existing bathymetric mapping technology into a small scaled autonomous watercraft. The watercraft is designed using hydrodynamic principles and simulation-based optimization process. The result of the study is the design of a watercraft hull form that provides a stable platform for bathymetric mapping in shallow waterbodies less than 100 m deep and waterflow velocities of less than 3 m/s. The watercraft has been tested to be capable of performing autonomous surveying missions in an area of up to 0.0125 km<sup>2</sup> with minor deviations.

## INTRODUCTION

Earth's surface is nearly 71% water, with most of it consisting of the ocean. This region however is barely explored, with less than 20% of it being accurately mapped. Bathymetric maps of shallower regions such as lakes and rivers are even more scarce as they cannot be accessed by large ships commonly used for bathymetric mapping [1]. An accurate knowledge of the underwater topography is a valuable asset as it can help humans to better assess geologic resources, predict hazards in navigation, perform aquatic habitat mapping, producing meteorological models as well as predicting global changes in the long term [2]. Waterbodies such as rivers, oceans or seas also pose a challenging environment for humans to navigate due to strong currents and waves. This makes surveillance as well as search and rescue missions in areas such as lakes or fast flowing rivers challenging and dangerous for humans. Furthermore, detailed bathymetric map of these areas is not readily available as these areas cannot be surveyed using the bathymetric mapping techniques commonly found on larger ships [3].

Current methods of oceanography including sensing of the ocean environment and meteorological surveys are conducted by ships, research vessels, buoys and satellites. Each of these methods comes with their own set of challenges. For satellites, there are many restrictions due to cover of clouds, spatial resolution and geographical/temporal coverage [4]. Research vessels and manned ships are expensive for conducting solely bathymetric mapping surveys, as well as having restriction in deployment areas. Moored buoys on the other hand lack self deployability and controllability making it an unsuitable option for bathymetric mapping purposes [5]. Due to all the mentioned factors, an autonomous watercraft would be the most suitable option for the purpose of bathymetric mapping due to their versatile capabilities for payload platform for sensor, autonomy as well as ease of deployment.

The potential application of the watercraft is also expanded with the development recent development of localization algorithms to track and land on a moving platforms for unmanned aerial vehicles (UAVs), allowing for system integration of sea and air monitoring systems [6]. This system can be made to be fully autonomous, working day and night to survey large areas and provide a constant stream of data to relevant agencies such as the navy or the maritime department to ensure the safety of transportation in these waterbodies [7].

With the advancement in electronics and microprocessors, small scale autonomous data collection devices can be produced at a lower cost compared to traditional data collection equipment. The production of a watercraft system that can brave the currents and waves will allow these shallower regions to be navigated through and surveyed using pre-set mission paths. Many autonomous multi-hulled watercrafts have been researched and developed over the past

decade. However, there has not been an implementation of such device at a small-scale with lengths below 1 m used in bathymetric mapping.

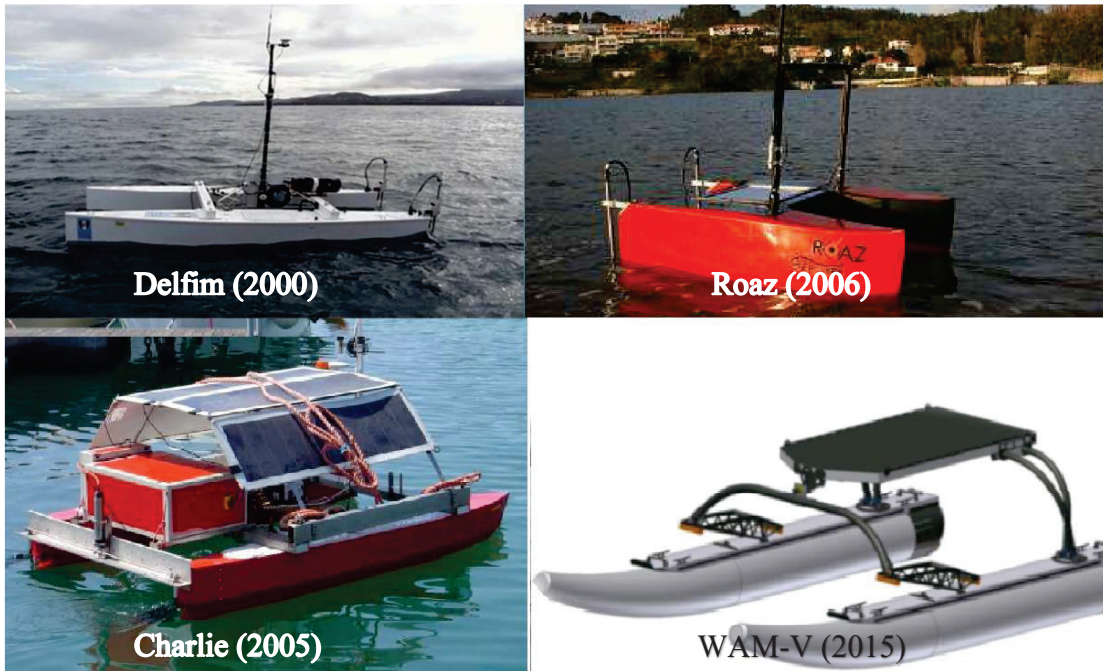


**FIGURE 1.** Autonomous watercrafts developed for oceanography.

Figure 1 shows some of the famous autonomous multi-hulled watercraft developed over the past decade used for marine research. Each of these watercrafts has been made for different research purposes:

1. Autonomous watercraft Delfim developed for marine data acquisition as well as communication relay in Lisbon 2000 [8].
2. Autonomous watercraft Roaz developed for autonomous missions and autonomous underwater vehicle testing [9].
3. Autonomous watercraft Charlie developed to study the microsurface layer of the sea in Genova 2005 [10].
4. Autonomous wave adaptive modular vessel developed for ocean observation in Osaka 2015 [11].

Although many autonomous watercrafts have been developed, there has not been an implementation of such device at a small-scale with lengths below 1 m used in bathymetric mapping. The implementation of these design incurs a substantial cost in manufacturability and deployability due to their large footprint.

In this project, a low cost and small scaled autonomous watercraft system is proposed for bathymetric mapping purpose. The watercraft system will be realized in the form of a multi-hulled, electrically powered platform which has increased stability even over strong currents. The watercraft will be controlled using an advanced microcontroller with a multitude of sensors such as global positioning system (GPS), an accelerometer and a magnetometer to maintain heading and provide accurate navigation data while a sonar sensor will be constantly recording depth information of the waterbody and stored in an onboard memory along with the coordinates where each data point is recorded. This data can then be extracted and analysed after each surveying mission.

## **WATERCRAFT DESIGN**

### **Mechanical Design**

The unmanned watercraft is designed to carry a combined payload of 2 kg including the propulsion and electronic systems. A twin-hull, also known as the catamaran configuration, is selected as it has better seakeeping and handling characteristics compared to other watercraft configurations [12]. The computer aided design (CAD) model of the

watercraft hull form was designed using SolidWorks. The hull form is further optimized through analyzing high pressure gradients region on the hull form using computational fluid dynamics (CFD) software Ansys Fluent, and further improving the streamline geometry in SolidWorks.

The size of the hull is designed within the constraints of 1 m<sup>2</sup> to be small enough for easy transportation and deployment, while being large enough to maintain stability and buoyancy while operating in shallow water bodies. The hull length is 0.8 m while the individual hulls are separated by 0.4 m and are 0.2 m wide. The electronic components are stored in the central fuselage that is positioned 0.1 m above the top of the hull and 0.35 m above the waterline. The total mass of the watercraft is 4.86 kg.

The hull of the watercraft is 3D printed using polylactic acid thermoplastics (PLA) material and is reinforced with two layers of fiber glass epoxy composite to strengthen and keep the hull watertight.



**FIGURE 2.** (a) First iteration of watercraft design. (b) Final iteration of the watercraft design.

Figure 2 shows the first and final iterations of the watercraft. The watercrafts were simulated in a multiphase environment of water and air, with varying freestream velocities. Ansys is then used to calculate the summation of pressure forces acting in the normal direction on the body of the hull to obtain the overall drag. The results are then used in Eq. (1) to identify the drag coefficient. The drag in air is neglected in the calculation as the contribution of drag from air is negligible compared to water [13].

$$F_D = \frac{1}{2} \rho A V^2 C_d \quad (1)$$

$F_D$  represents the drag acting on the hull, while  $\rho$  represents the density of the fluid medium, which will be water.  $A$  represents the wetted surface area where the hull is in contact with the water and is measured from the CAD model of the hull.  $V$  represents the net velocity of the watercraft on the water surface.  $C_d$  represents the drag coefficient of the hull, which is a constant value for each hull design used to determine the drag acting on the hull at different velocities.

From Table 1, it can be observed that there is a 15% decrease in the frictional coefficient after the optimization process. This results in a hull form with a low drag coefficient, making it better suited for long distance missions during the bathymetric mapping process. From Figure 3, it can be observed that the drag force increases to the square of the velocity of the hull, and requires a large amount of thrust to propel the watercraft at higher velocities, with a total of 2500 N of drag when hull (a) is travelling at 13 m/s, while only requiring 1750 N of thrust for hull (b). The optimized hull shows a significant decrease in required thrust.

TABLE 1. Simulation results of hull drag

Hull	Wetted Surface Area, $A$ ( $m^2$ )	Velocity, $V$ (m/s)	Drag Force, $F_d$ (N)	Drag Coefficient, $C_d$	Average Drag Coefficient, $C_d$
Hull (a)	0.146	1	15.2	0.208	0.203
		2	58.7	0.201	
		3	130.7	0.199	
Hull (b)	0.121	1	10.6	0.175	0.173
		2	42.8	0.177	
		3	91.5	0.168	

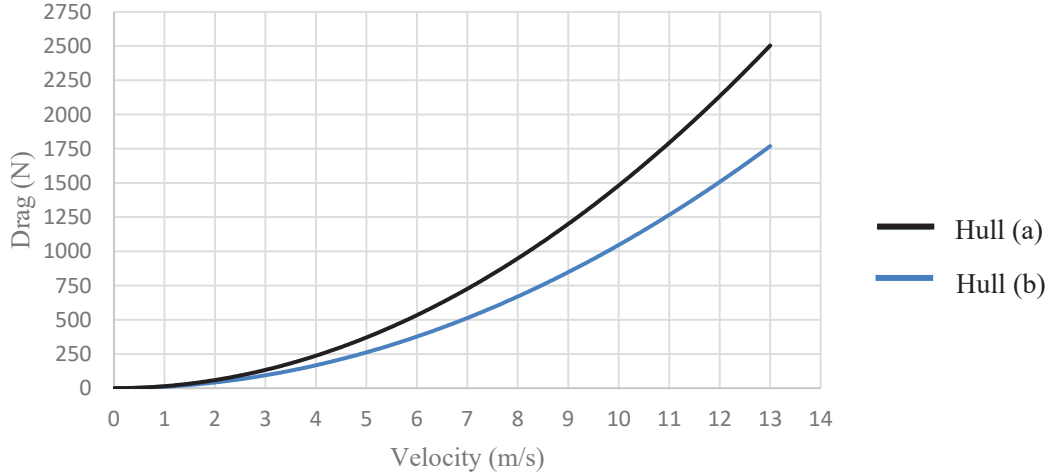


FIGURE 3. Graph of comparison in drag against velocity of the watercraft using hull (a) and hull (b).

### Propulsion System

The watercraft is propelled using a twin brushless-motor configuration, with a motor on each hull. The direction of the watercraft is controlled through differential thrust from the separate motors. The motor used is a 3370-kV bi-directional brushless motor paired with a 3-blade propeller with 20 mm diameter and 8 mm pitch. The selection of the motor and propeller combination is based on similar functional configuration [11] as there are limited resources on the performance of small-scale propellers.

To power the propulsion system, a 4S, 3500 mAh lithium-polymer (LiPo) battery is used. Separate 80A electronic speed controllers (ESCs) are used to control the motors, however, batteries with larger capacity can be used when surveying larger areas. To evaluate the performance of the selected motor-propeller combination, a test rig is produced to measure the thrust produced.

Figure 3 shows the experimental setup whereby the motor is connected to a levering arm. The thrust produced by the motor causes the levering arm to exert an equivalent amount of force on the weighing scale. The motor is tested at different percentage levels of thrust. As the experiment is performed in air, the equivalent amount of thrust in water can be identified using Eq. (3) derived from Eq. (2).

$$F_p = \frac{1}{2} \rho A (V_e^2 - V_0^2) \quad (2)$$

$$F_{pw} = \frac{\rho_w}{\rho_a} F_{pa} \quad (3)$$



**FIGURE 4.** Experimental setup to identify the thrust produced from the motor and propeller.

$F_{pw}$  and  $F_{pa}$  represents the thrust produced by the motor in water and air respectively.  $V_e$  and  $V_0$  represents the exit velocity and the freestream velocity of the fluid across the propeller.  $A$  represents the area of the propeller.  $\rho_w$  and  $\rho_a$  represent the densities of water and air respectively. As the area and velocities are equal when in air and in water, the thrust produced by the motor in water can be equated to the product of the ratio of density of water to density of air and the thrust produced by the motor in air [14].

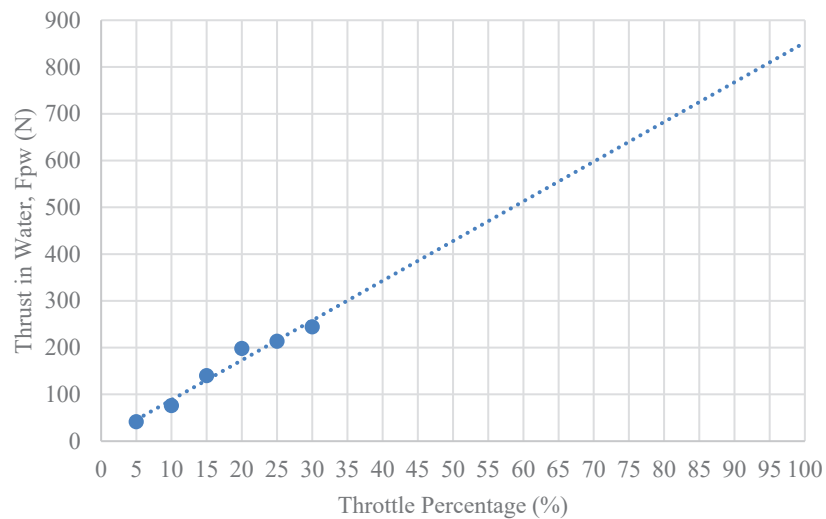


**FIGURE 5.** Experimental results of thrust produced by a single motor, extrapolated to 100% throttle.

From Figure 5, it can be observed that the amount of thrust increases linearly against the throttle percentage. At 5% throttle, the motor was already able to produce 41 N of thrust, which was close to the frictional drag acting on the hull at 2 m/s of 42.8 N. The motors could produce up to 244 N of thrust at 30% throttle, which was enough for the watercraft to travel at 4.4 m/s with only one motor. The experiment was conducted to up to 30% throttle only as the propulsion system begins to heat up excessively at higher throttle percentage without the aid of the water-cooling system. The maximum theoretical combined thrust from the extrapolated graph is 850 N. Comparing the thrust required and thrust available from Figure 4 and Figure 5, the watercraft can travel at up to 12.7 m/s at maximum thrust at full throttle using both motors.

The propulsion system is positioned 5 cm below the waterline of the hull to ensure complete submersion of the propellers as the propeller loses a significant amount of efficiency when operating in air. The propulsion system is

water-cooled passively using the pressure under the hull of the watercraft to pump water across the heat sinks of the ESCs and brushless motors.

## Controls and Communications System

To control the automatic waypoint mission of the watercraft, a computer system is used. A Pixhawk 4 controller is used as the main processing unit. An open-sourced firmware, ArduRover v3.5.2 is uploaded onto the controller to perform all the signal processing.

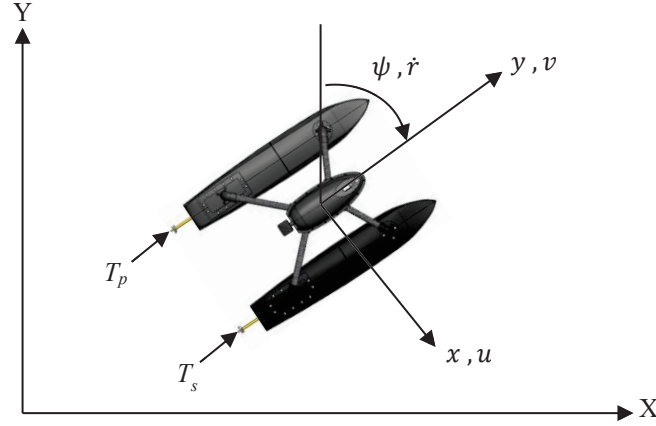


FIGURE 6. Coordinate system of the watercraft.

To create an autonomous control system for the multi-hulled watercraft, a mathematical model first needs to be derived based on the design of the watercraft used to perform simulations. Figure 6 shows a model produced for a multi-hulled watercraft and its coordinate system based on the MMG standards [15]. The position and orientation are described by a vector  $R = [x \ y \ \psi]$ , while the state vector is described by the vector  $s = [u \ v \ r]$ . The thrust produced by the left and right motors are denoted by  $T_p$  and  $T_s$ . The P and S subscripts represent the port and starboard motors. The controller uses a PID controller describe in Eq. (4) to take in control setpoints of heading angle and velocity to produce a set of outputs for the motor speed [16].

$$\tau_{PID} = K_p(\psi_d - \psi) - K_d(r_d - r) + K_i \int_0^t (r_d - r) dt \quad (4)$$

A GPS module, Ublox NEO-M8N, is connected to the controller to determine the positional coordinates of the watercraft. Using the coordinates, the controller then computes the output signals to control the motion of the watercraft to follow the preplanned waypoints.

A FrSky tfr8 radio receiver operating at 2.4 GHz is connected to the controller to allow users to remotely control the watercraft using a Taranis QX7 radio transmitter during setup and retrieval. A pair of telemetry module operating at 433 MHz is connected to the controller and ground control laptop individually for monitoring the status of the watercraft remotely using a ground control software, Mission Planner. The software is used to monitor the position, battery level, controller outputs, velocity and heading of the watercraft. It can also be used to override control parameters of the watercraft or modify the mission waypoints.

All electronic components share the same power source used in the propulsion system. A buck converter is used to lower the input voltage of the LiPo battery to 5 v to power the controls and communication system.

## Bathymetric Sensor integration

The bathymetric sensor used in this research is the DST800 Airmar Triducer. It is a SBES that is capable of measuring a depth range of up to 100 m with a data update rate of 1 Hz. It is powered at a 10 to 25 v range and is powered directly using the same power supply from the propulsion system. This sensor is selected as it is cost effective and suited for surveying shallower water bodies such as lakes and rivers.

The sensor output is in the NMEA0183 format and is converted to a digital signal using a RS-485 TTL converter. The converted signal is then recorded by the controller and is written into an SD card which will be collected after the mission is completed by the watercraft. The sensor is mounted 0.075 m below the waterline of the hull to ensure complete submersion even on disturbed water surfaces.

The total cost for the complete system is summarized in Table 2. Maintenance cost of the watercraft is minimal with only the need for occasional replacement of the shaft lubricant and propellers. Operating cost of the watercraft includes the charging of the Li-Po battery in the watercraft as well as the transmitters. Optional cost includes multiple or larger capacity Li-Po batteries for larger scale surveying missions.

**TABLE 2.** Project cost breakdown.

<b>Item</b>	<b>Cost</b>
Watercraft Frame	50
Brushless motors	250
Electronic speed controllers	200
Propellers and shaft	50
Li-Po battery	50
Open source control board	500
GPS receiver	200
Echosounder	1200
Analog signal converter	950
Battery charger	100
7 Channel radio transmitter and receiver	500
<b>TOTAL COST</b>	<b>4050</b>

## **BATHYMETRIC SURVEYING METHODOLOGY**

### **Bathymetric Survey Planning**

The planning of the bathymetric survey in this research is based on the IHO Standard for Hydrographic Surveys (S-44). The surveys performed by the watercraft is under the classification of Order 1a and 1b, where areas of survey are shallower than 100 m for both orders. A full sea floor search is required in 1a while not required in 1b. A full sea floor search requires a systematic identification of features, whether manmade or not, that is projecting 2 m from the sea floor that may endanger navigation on the water surface [17].

The total allowable horizontal uncertainty of the survey is 5 m + 5% of depth for both Order 1a and 1b, while the total allowable vertical uncertainty is 0.5 m. The GPS module used has a specified positional accuracy of 2 m circular error probable (CEP). The horizontal uncertainty is within acceptable range, however the vertical uncertainty from the depth sensor is unspecified in the manufacturers data sheet. A benchmark test is performed using varying water depths to determine the uncertainty of the depth sensor. The depth sensor has shown a consistent uncertainty of less than 0.5% from the 0.5 to 1.5 m range. The sensor shows reliability in this range but the uncertainty of the full range of the sensor could not be determined with available equipment.

The distance between each data collection point should be at least 2 m from each other for Order 1a and 5 m for Order 1b. The Mission Planner software is used to plan the data collecting region. The watercraft will be programmed to follow a zig-zagging waypoint pattern with a 2 m spacing between each pass in Order 1a, while the spacing for Order 1b is 5 m, as shown in Figure 7. The watercraft will maintain a 1 m/s velocity along the surveying mission path for Order 1a and 2 m/s for Order 1b.

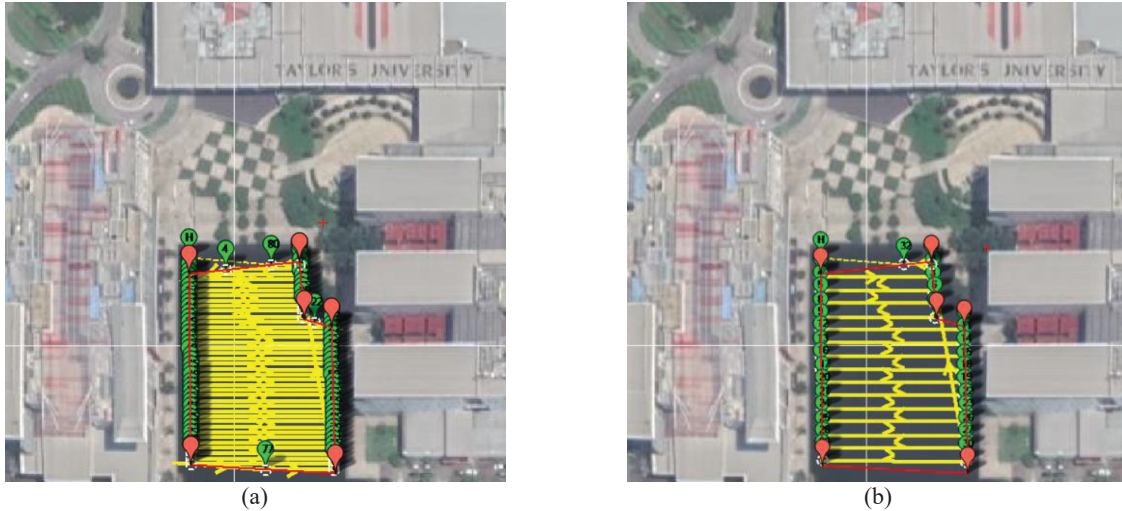


**FIGURE 7.** Survey mission path planned for Taylor’s University lake. (a) Planned mission for Order 1a, with spacing between survey lines of 2 m. (b) Planned mission for Order 1b, with spacing between survey lines of 5 m.

## Data Processing

The data collected from the survey is previewed in Mission Planner to identify any erroneous data. Data points that show a large spike in reading compared to neighboring data are flagged and excluded from the bathymetric map. A copy of the original data is saved as a metadata file that will accompany the final bathymetric map during the final export.

The revised data is then tabulated according to the latitude, longitude and the water depth and saved as a .txt file. It is then exported into ReefMaster underwater mapping software. Compensation for tidal adjustment is added using the time of survey and is automatically computed by the software.

Both 2D and 3D maps are generated using the software and are exported as ESRI Shapefile format for the 2D contour map and ESRI Grid format for the 3D bathymetric map, which can be accessed by other geographical information system (GIS) applications [18].

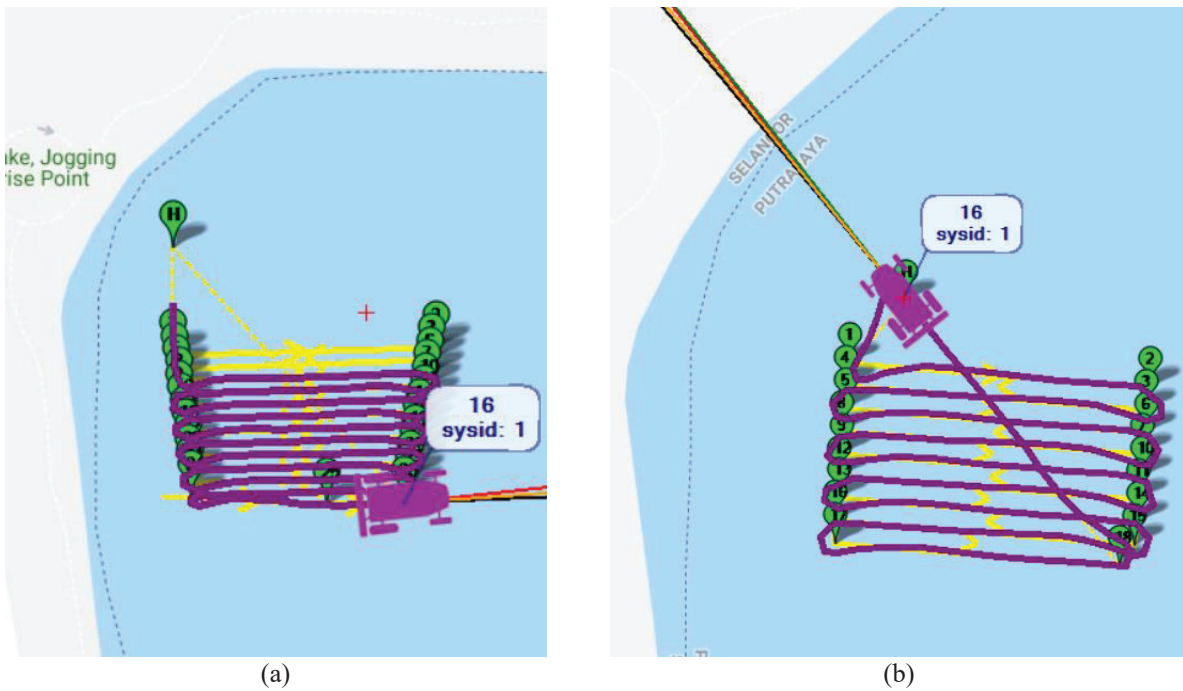
## TEST RESULTS

### Automatic Mission Test

To perform the test, an automatic waypoint mission was programmed to assess the performance of the controller of the watercraft. The actual trajectory of the watercraft is compared with the target trajectory. The test was performed during in similar water conditions on fine weather with minimal winds to ensure similar operating conditions. The pre-mission checklist was performed to ensure the hardware are in the same condition for each test. After each test, the watercraft is checked for any leaks or changes in hardware.

From the test, key performance data has been recorded, including control and communication functions, waypoint mission accuracy, watercraft range, as well as PID controller performance.

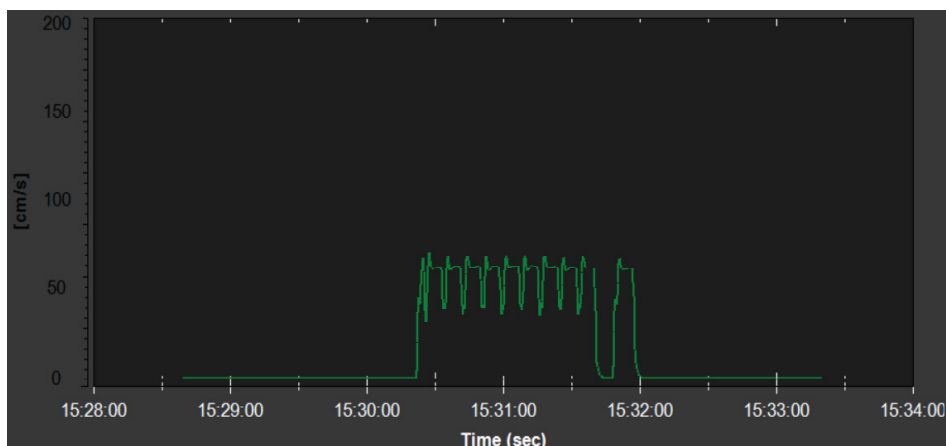
The test was performed at Putrajaya Lake, with a gridded waypoint mission programmed at 5 m spacing between each gridline. The watercraft was manually controlled to start the mission at the center of the lake. The starting position is set as the home position before switching over to auto mode for the waypoint mission to begin.



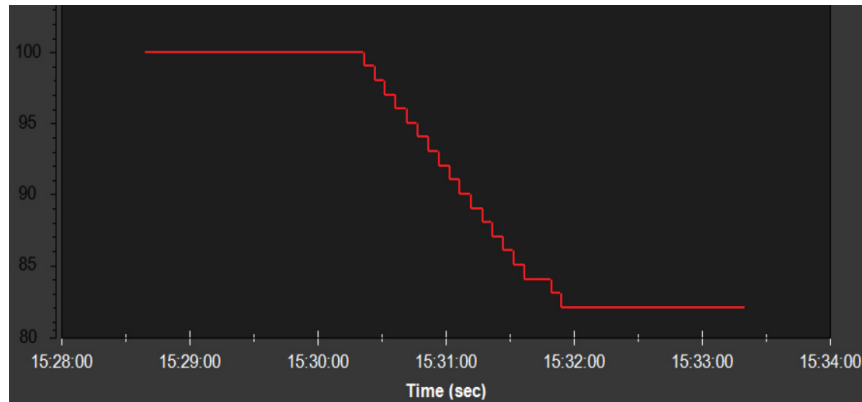
**FIGURE 8.** Automatic waypoint mission performed at Putrajaya Lake, green labels represent individual waypoints, yellow lines represent the target trajectory while purple lines represent the actual trajectory. (a) Mission without any tuning of PID values. (b) Mission after tuning of PID values.

Figure 8 shows the waypoint mission log at the lake. The watercraft was overshooting due to the untuned PID gains, causing it to miss several waypoints at the beginning. Although it has no problems following the straight trajectories, the watercraft tend to overshoot when making turns. The PID values are tuned based on the results of the test run, where the proportional gains are lowered to decrease overshoot, while the derivative gains are increased to increase damping effect for better turning [19]. After tuning the PID values, the watercraft was able to follow the target trajectory and reach each of the waypoints, before completing the waypoint mission and returning to its home coordinates.

The mission speed was set at 0.5 m/s and the controller has shown to be able to keep up with the target speed most of the time throughout the mission. However, there were some stalling that occurred around time 15:31:45 as shown in Figure 9.



**FIGURE 9.** Velocity of watercraft during the mission with tuned PID gains.



**FIGURE 10.** Remaining battery percentage during the mission with tuned PID gains.

The total distance of the mission is 0.56 km and the battery level has depleted to 82% after the mission as observed in Figure 10. Excluding a threshold of 20% battery percentage safety margin for return to launch of the watercraft, the total range of the watercraft available for autonomous mission is about 2.5 km. The total area covered by this range for surveys of Order 1a is 0.005 km<sup>2</sup> and 0.0125 km<sup>2</sup> for Order 1b. As the sizes of lakes range from 0.02 km<sup>2</sup> up to 1000 km<sup>2</sup>, the capacity of the battery used needs to be increased for larger surveying missions. However, for smaller regions such as ponds or rivers, the current configuration would prove to be capable of completing the survey in a single mission.

## CONCLUSION

In this research, a complete system integration for a small-scaled autonomous watercraft has been produced as a platform for bathymetric mapping surveys. Using hydrodynamic principles and simulation-based optimization process, an optimized hull form has been produced, with a low drag coefficient of 0.173. An appropriate propulsion system has been integrated with the watercraft that is able to propel the watercraft up to 12.7 m/s. The total range available in a single charge for the watercraft using a LiPo powered source of 3500 mAh is up to 2.5 km while the area covered is 0.005 km<sup>2</sup> for Order 1a and 0.0125 km<sup>2</sup> for Order 1b. The implementation of the controls and communication system, consisting of on-board controller, GPS module, telemetry and radio communication systems, the watercraft is able to be controlled manually for mission setup as well as complete autonomous waypoint following during surveying missions. The watercraft is monitored remotely using a ground control software on a laptop during the mission. The implemented controls system with a tuned PID controller is able to complete waypoint missions with minimal deviation from the predefined waypoint trajectories. To improve the performance of the watercraft, the propulsion system as well as the power source on the watercraft can be changed. The current brushless motor of 3370-kV can be decreased to a lower kV to decrease the RPM of the motor while increasing the torque as the survey mission of the watercraft is performed at a low velocity. With a higher torque, the propeller size can be increased, allowing for higher velocities at lower RPM, thus further increasing efficiency. A larger battery capacity can also be used to further improve the range of the watercraft, allowing for larger area of survey. Future work of this research is to implement the SBES sensor to the produced autonomous watercraft platform and perform bathymetric surveys. Although the watercraft is capable of autonomous missions, there is a lack of sensors for obstacle avoidance, causing the need of human intervention in certain scenarios. The completed project will have a competitive edge in surveillance of waterbodies compared to full scale research vessels due to its low cost and deployability. The fully autonomous watercraft can also be used in other waterbody related research areas as the electronics and software are fully open sourced, allowing other equipment to be installed for data collection.

## ACKNOWLEDGEMENTS

This project is funded by School of Engineering, Taylor's University. The authors of this paper would also like to acknowledge FourFang Sdn. Bhd. for providing the equipment used in this research.

## REFERENCES

1. P. Weatherall, K. M. Marks, M. Jakobsson, T. Schmitt, S. Tani, J. E. Arndt, M. Rovere, D. Chayes, V. Ferrini, and R. Wigley, "A new digital bathymetric model of the world's oceans," *Earth and Space Science*, vol. 2, no. 8, pp. 331–345, 2015.
2. M. Włodarczyk–Sielicka and A. Stateczny, "Clustering Bathymetric Data for Electronic Navigational Charts," *Journal of Navigation*, vol. 69, no. 5, pp. 1143–1153, 2016.
3. J. J. Becker, D. T. Sandwell, W. H. F. Smith, J. Braud, B. Binder, J. Depner, D. Fabre, J. Factor, S. Ingalls, S.-H. Kim, R. Ladner, K. Marks, S. Nelson, A. Pharaoh, R. Trimmer, J. Von Rosenberg, G. Wallace, and P. Weatherall, "Global Bathymetry and Elevation Data at 30 Arc Seconds Resolution," *Marine Geodesy*, vol. 32, no. 4, pp. 355–371, 2009.
4. R. P. Dziak, C. G. Fox, A. M. Bobbitt, and C. Goldfinger, "Bathymetric Map of the Gorda Plate: Structural and Geomorphological Processes Inferred from Multibeam Surveys," *Marine Geophysical Researches*, vol. 22, no. 4, pp. 235–250, 2001.
5. L. Mayer, M. Jakobsson, G. Allen, B. Dorschel, R. Falconer, V. Ferrini, G. Lamarche, H. Snaith, P. Weatherall, L. Mayer, M. Jakobsson, G. Allen, B. Dorschel, R. Falconer, V. Ferrini, G. Lamarche, H. Snaith, and P. Weatherall, "The Nippon Foundation—GEBCO Seabed 2030 Project: The Quest to See the World's Oceans Completely Mapped by 2030," *Geosciences*, vol. 8, no. 2, p. 63, 2018.
6. K. Wang, S. K. Phang, Y. Ke, X. Chen, K. Gong, and B. M. Chen, "Vision-aided tracking of a moving ground vehicle with a hybrid UAV," in *2017 13th IEEE International Conference on Control & Automation (ICCA)*, 2017, pp. 28–33.
7. X. Chen, S. K. Phang, M. Shan, and B. M. Chen, "System integration of a vision-guided UAV for autonomous landing on moving platform," in *2016 12th IEEE International Conference on Control and Automation (ICCA)*, 2016, pp. 761–766.
8. J. Alves, P. Oliveira, R. Oliveira, A. Pascoal, M. Rufino, L. Sebastiao, and C. Silvestre, "Vehicle and Mission Control of the DELFIM Autonomous Surface Craft," in *2006 14th Mediterranean Conference on Control and Automation*, 2006, pp. 1–6.
9. H. Ferreira, A. Martins, A. Dias, C. Almeida, J. M. Almeida, and E. Silva, "ROAZ Autonomous Surface Vehicle design and implementation," *Robotica*, vol. 24, no. 1, pp. 250–269, 2006.
10. M. Caccia, M. Bibuli, R. Bono, G. Bruzzone, G. Bruzzone, and E. Spirandelli, "Unmanned Marine Vehicles at CNR-ISSIA," *IFAC Proceedings Volumes*, vol. 41, no. 2, pp. 3070–3075, 2008.
11. J. Pandey and K. Hasegawa, "Study on manoeuvrability and control of an autonomous Wave Adaptive Modular Vessel (WAM-V) for ocean observation," in *2015 International Association of Institutes of Navigation World Congress (IAIN)*, 2015, pp. 1–7.
12. M. Kandasamy, P.-C. Wu, S. Zalek, D. Karr, S. Bartlett, and L. Nguyen, *CFD based Hydrodynamic Optimization and Structural Analysis of the Hybrid Ship Hull*. 2014.
13. S. Percival, D. Hendrix, and F. Noblesse, "Hydrodynamic optimization of ship hull forms," *Applied Ocean Research*, vol. 23, no. 6, pp. 337–355, 2001.
14. J. F. Groeneweg and L. J. Bober, "NASA advanced propeller research," 1988.
15. H. Yasukawa and Y. Yoshimura, "Introduction of MMG standard method for ship maneuvering predictions," *Journal of Marine Science and Technology*, vol. 20, no. 1, pp. 37–52, 2015.
16. A. Francescutto, "Mathematical Modeling of Roll Motion of a Catamaran In Intact And Damage Conditions In Beam Waves," *The Tenth International Offshore and Polar Engineering Conference*. International Society of Offshore and Polar Engineers, Seattle, Washington, USA, p. 7, 2000.
17. "IHO Transfer Standard for Digital Hydrographic Data," *International Hydrographic Bureau MONACO*, vol. 3, no. 1, pp. 15–20, 2014.
18. R. J. J. Dost and C. M. M. Mannaerts, "Generation of lake bathymetry using sonar, satellite imagery and GIS," in *Proceedings of the 2008 ESRI international user conference: GIS, Geography in action. San Diego, Florida*, 2008.
19. Q.-G. Wang, T.-H. Lee, H.-W. Fung, Q. Bi, and Y. Zhang, "PID tuning for improved performance," *IEEE Transactions on control systems technology*, vol. 7, no. 4, pp. 457–465, 1999.